Cooperative Cell Outage Detection in Self-Organizing Femtocell Networks

Wei Wang, Jin Zhang, Qian Zhang
Department of Computer Science and Engineering,
Hong Kong University of Science and Technology
Email: {gswwang, jinzh, qianzh}@ust.hk

***Abstract*—The vision of Self-Organizing Networks (SON) has been drawing considerable attention as a major axis for the development of future networks. As an essential functionality in SON, cell outage detection is developed to autonomously detect macrocells or femtocells that are inoperative and unable to provide service. Previous cell outage detection approaches have mainly focused on macrocells while the outage issue in the emerging femtocell networks is less discussed. However, due to the two-tier macro-femto network architecture and the small coverage nature of femtocells, it is challenging to enable outage detection functionality in femtocell networks. Based on the observation that spatial correlations among users can be extracted to cope with these challenges, this paper proposes a Cooperative femtocell Outage Detection (COD) architecture which consists of a trigger stage and a detection stage. In the trigger stage, we design a trigger mechanism that leverages correlation information extracted through collaborative filtering to efficiently trigger the detection procedure without inter-cell communications. In the detection stage, to improve the detection accuracy, we introduce a sequential cooperative detection rule to process the spatially and temporally correlated user statistics. In particular, the detection problem is formulated as a sequential hypothesis testing problem, and the analytical results on the detection performance are derived. Numerical studies for a variety of femtocell deployments and configurations demonstrate that COD outperforms the existing scheme in both communication overhead and detection accuracy.**

I. Introduction

Self-Organizing Networks (SON) have recently been recognized as an attractive paradigm for the next-generation cellular systems by standardization bodies [1] [2], which enable autonomic features in networks, including self-configuration, self-optimization and self-healing [3] [4]. In the self-healing mechanism, cell outage detection is considered to be one of the fundamental functionalities, which aims to autonomously detect cells in an *outage* state, i.e., cells that are inoperable and cannot provide any service due to hardware failures, software failures or even misconfigurations [2]. Cell outage often results in decreased capacity and coverage gap. Such degraded performance leads to high user churn rate and high operational expenditures [5]. However, detecting outaged cells is non-trivial. The outaged cells cannot be detected by Operations Support System (OSS) when the detection systems of the outaged cells malfunction [6]. In addition, it is difficult for the cellular system management functions to detect outaged cells directly when the outage is caused by misconfigurations. Identifying these outaged cells usually requires unplanned site visits and may take hours or even days [5]. To reduce manual costs and detection delay, the cell outage detection function is proposed in [2] to automatically identify the outaged cells by users' performance statistics analysis.

Most, if not all, previous cell outage detection approaches have focused on macrocells [7] [8]. However, traditional macrocell networks are likely to be supplemented with smaller femtocells deployed within homes and enterprise environments in the next-generation cellular networks [9], where outage occurs more frequently because of inappropriate indoor human interactions and unplanned deployment of large numbers of femto access points (FAPs). Unfortunately, when applied in femtocell networks, existing macrocell outage detection works fall short due to the following distinct features of femtocell networks.

- **Dense deployments**. Since there are normally tens or hundreds of femtocells deployed within a macrocell, the number of femtocells is much larger compared with macrocells. The centralized statistics analysis adopted by macrocell outage detection approaches [7] [8] will involve high communication overhead if applied directly in femtocell networks, which will degrade the femtocell service.
- **Vertical handover**. Femtocell users can vertically handover between femtocell and macrocell. However,this vertical handover issue is not considered in the existing macrocell outage detection approaches [7] [8]. In the two-tier femto-macro cellular networks, when a femtocell outage occurs, its users may handover to macrocell and be unaware of the outage. This can be misleading in the user statistics analysis.
- **Sparse user statistics**. Unlike macrocell with large coverage, small scale indoor femtocell usually only supports a few active users (typically 1 to 4 active mobile phones in a residential setting [10]). Macrocell approaches [7] [8], which are based on user statistics within one cell, however, fall inaccurate due to the sparsity of user statistics with high uncertainty caused by severe indoor shadowing fading. In the worst case, femtocell with small coverage may have no active users in certain time slots, leading to the failure of these algorithms.

To overcome the aforementioned challenges in femtocell networks, we propose an efficient detection architecture, referred to as *COD* (Cooperative femtocell Outage Detection), which consists of an intra-cell trigger stage and an inter-cell detection stage. The core idea of this architecture includes the following considerations: 1) To reduce communication overhead, the trigger procedure runs on each FAP in a distributed manner without any inter-cell communications. We design a low cost mechanism to trigger the detection for possible outage femtocell via long term passive monitoring users' *Reference Signal Received Power* (RSRP) statistics. The RSRP statistics are user's basic physical layer measurements on the linear average of the downlink reference signals across the channel bandwidth [11]. 2) The trigger decisions are based on spatial correlations among users' RSRP statistics, rather than disconnected devices [12] [13] or neighbor list [7] in traditional approaches. The correlations of RSRP statistics are leveraged to distinguish the vertical handover case and the outage case. 3) To cope with the data sparsity issue, a detection rule enables neighboring femtocells to cooperatively detect outaged femtocells over a certain period of time, so as to expand statistics over the space domain and the time domain to obtain enough information. A data fusion rule is used to process the statistics to make a final decision.

According to the above three guidelines, the key problems behind this architecture are *how to extract correlations of intra-cell RSRP statistics in space domain* and *how to extract correlations of inter-cell RSRP statistics in space and time domains*. We leverage *collaborative filtering* [14] and *sequential detection* model [15] to tackle the two problems respectively. In the trigger stage, each FAP predicts the current normal statistics of its neighboring cells using collaborative filtering. The trigger decision is made based on the comparison between the predicted statistics and real statistics. In the detection stage, statistics within an area, referred to as *cooperation range*, are processed at the macrocell base station (MBS) via the sequential detection model. The spatial characteristics of statistics are exploited to derive the minimal time that is needed to make a final decision.

To the best of our knowledge, this paper is the first work to explore the outage detection problem in the context of femtocell networks. The main contributions of this work can be summarized as follows:

- This paper proposes a correlation based outage detection architecture in consideration of the unique challenges in femtocells. This architecture can be used as a general framework for designing femtocell outage detection schemes.
- A distributed trigger mechanism is designed to reduce the communication overhead and to address the vertical handover issue. The trigger mechanism exploits the spatial correlations of RSRP statistics via collaborative filtering. The extracted spatial correlations enable the trigger mechanism to make a trigger decision without any inter-cell communication overhead.
- A cooperative detection rule is proposed to cope with the data sparsity issue by extracting both spatial and temporal correlations of RSRP statistics over multiple femtocells. The detection problem is formulated as a sequential hypothesis testing problem to minimize the detection delay.
- We identify the impacts of the cooperation range and the user density on detection performance by deriving closed-form expressions. Analytical results show that the expected detection delay is inversely proportional to the user density and the cooperation area, and is independent of the FAP's transmission power.
- We conduct extensive numerical studies, and the evaluation results show that the proposed approach outperforms the conventional method in terms of communication cost as well as detection accuracy.

The rest of the paper is organized as follows. Section II describes the system model. Section III illustrates the rationale of the proposed COD architecture. In Section IV, the trigger mechanism used in the trigger stage of COD is introduced. Section V formulates the cooperative outage detection problem in the detection stage of COD as a sequential hypothesis testing problem and derives analytical results. Numerical results are presented in Section VI. Related works are reviewed in Section VII. Finally, Section VIII concludes the paper.

II. System Model

In this section, we introduce the network model, the user model and the channel model.

A. Network Model

We consider a typical two-tier femtocell network architecture where a set of femtocells $\mathcal{F} = \{1, ..., F\}$ are overlaid on a macrocell. Femtocell f operates under FAP f. A femtocell experiences outage with certain probability in the process of operation. The outaged FAP cannot transmit or receive any signal. We assume that the locations of FAPs are known to the MBS. We also assume that the transmission powers of FAPs are constant during the detection process. FAPs transmit reference signals periodically in the downlink. The reference signals, which facilitate user's channel measurements (e.g., RSRP measurement), are sent back to the FAPs as feedback messages.

B. User Model

The locations of the users are unknown. The users transmit or receive data from their associated FAPs, and periodically report the RSRP statistics of all neighboring cells to their associated FAPs, providing guidance in handover and cell reselection decisions. We assume that the users in an area A follow a Poisson point process with density ρ, i.e., $n_A \sim Poi(n; \rho|A|)$, where n_A is the number of users within an area A.

C. Channel Model

The channel gains of a user u to an FAP f are determined based on the the model described in [16]:

$$h = (\frac{d_o}{d_{u,f}})^a e^{X_{u,f}} e^{Y_{u,f}}, \tag{1}$$

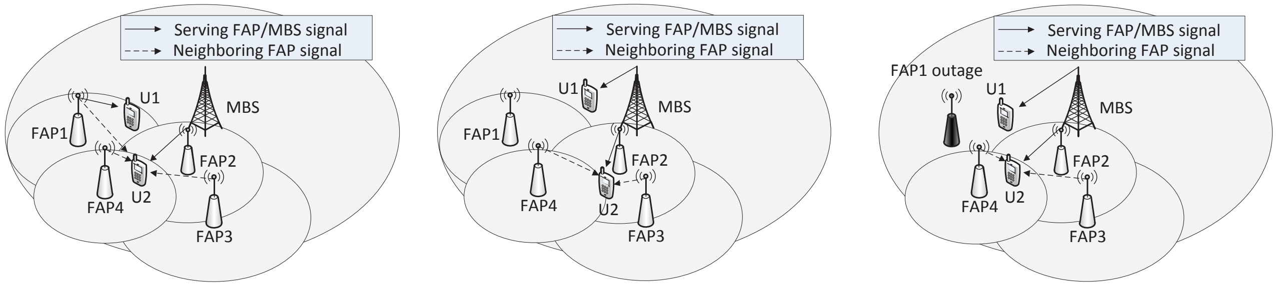

	FAP1	FAP2	FAP3	FAP4
U1	1(+)	0	0	0
U2	1(-)	1(+)	1(-)	1(+)

RSRP Statistics

(a) Normal case

	FAP1	FAP2	FAP3	FAP4
U1	0	0	0	0
U2	0	1(+)	1(+)	1(-)

RSRP Statistics

(b) Vertical handover case

	FAP1	FAP2	FAP3	FAP4
U1	0	0	0	0
U2	0	1(+)	1(-)	1(+)

RSRP Statistics

(c) Outage case

Fig. 1: Cases in femtocell outage detection

where d_o is the reference distance (e.g., 1 m), $d_{u,f}$ the distance between the FAP f to the user u, and a the path loss exponent. $e^{X_{u,f}}$ and $e^{Y_{u,f}}$ are shadowing fading factor and multi-path fading factor, respectively. The shadowing fading follows a Gaussian distribution described by $X_{u,f} \sim \mathcal{N}(0, \sigma), \forall u, f$. The multi-path fading is modeled by Rayleigh fading with zero mean, and thus $\mathbb{E}[e^{Y}_{u,f}] = 0$.

We assume that shadowing fading effects are independent over time. Regarding this assumption, the RSRP statistics of a user are independent random variables. Note that all RSRP statistics can be characterized by Eq. (1). As such, the RSRP s-tatistics at u are independent and identically distributed (i.i.d.), and thus can be approximated as a Gaussian distribution using the *Central Limit Theorem* (CLT). Then, the distribution can be given as [17]:

$$r_u \sim \begin{cases} \mathcal{N}(N_o, \frac{{N_o}^2}{M}) & \mathcal{H}_0 \\ \mathcal{N}(P_u + N_o, \frac{(P_u+N_o)^2}{M}) & \mathcal{H}_1 \end{cases} \tag{2}$$

where r_u is user u's RSRP statistics, P_u the received signal strength at user u, N_o the noise power, and M the number of signal samples, e.g., 5×10^3 /ms for 5 MHz band. $\mathcal{H}_0$ stands for the outage case and $\mathcal{H}_1$ for the normal case.

III. Rationale of The COD Architecture

In this section, we first use a motivated example to illustrate the requirements of femtocell outage detection and our observation. Then, we propose the COD architecture.

A. *Requirements of Femtocell Outage Detection*

Due to the unique features of the femtocell networks, the following requirements need to be imposed when designing a femtocell outage detection architecture.

First, the communication overhead should be minimized to preserve the capacity of the femtocells. This can be achieved by: 1) designing a distributed trigger mechanism that involves much less communication overhead compared with the detection stage, and 2) minimizing the detection time (i.e., detection delay) of the detection stage.

Second, the effectiveness of the outage detection should be guaranteed even in the event of vertical handover. Fig. 1 illustrate the vertical handover issue in the two-tier femto-macro architecture. In the normal case (Fig. 1(a)), all femtocells operate normally and the user U1 is associated with the femtocell FAP1. Then, U1 vertically handovers to the MBS, which is caused by the movement of U1 (Fig. 1(b)) or the outage of FAP1 (Fig. 1(c)). Unfortunately, many existing approaches cannot differentiate the outage case (Fig. 1(c)) from the vertical handover case (Fig. 1(b)). In wireless LAN diagnosis or fault detection, the detection procedures are usually triggered by disconnected users [12] [13], which is not applicable in femtocell outage detection since users can handover to macrocell when there is no available femtocell around (e.g., Fig. 1(c)). Neighbor list based approaches [7] [18] are proposed to detect outages by looking at the changes in the network topology. Whereas, when applied in femtocell outage detection, the neighbor list based approaches derive the same network topology for Fig. 1(b) and Fig. 1(c), and thus cannot distinguish the outage case from the vertical handover case. Thus, a trigger mechanism that can differentiate these two cases is required.

Another unique feature of femtocell is that, the indoor femtocell supports much fewer users compared with the macrocell. Since severe indoor shadowing fading results in fluctuation of user statistics, analysis based on the sparse user statistics may lead to inaccurate results. To design a robust detection rule, the accuracy should be guaranteed even when femtocells have very few users.

B. *Observation*

To design a femtocell outage detection architecture that achieves the aforementioned requirements, we further investigate the spatio-temporal correlations in RSRP statistics. In

Fig. 1, U2 keeps moving in three cases, while U1 remains in the same location in the normal case and the outage case but moves away from FAP1 in the vertical handover case. The tables in Fig. 1 show the corresponding RSRP statistics, which are classified into three levels: 1(+) for strong received signal from a certain FAP, 1(-) for weak received signals, and 0 for no received signal. Comparing Fig. 1(a) and Fig. 1(c), U2's RSRP statistics from FAP2-FAP4 are the same while the RSRP statistics from FAP1 are different. A previous study [19] shows that users in close proximity have similar signal statistics, and the estimation of location similarity is more accurate when there are more FAPs nearby. Then, we can infer that the locations of U2 in Fig. 1(a) and Fig. 1(c) are probably close, and thus the RSRP from FAP1 should be similar in the two figures if FAP1 is normal in Fig. 1(c). Thus, the difference of RSRP from FAP1 in the two figures indicates that FAP1 may experience outage in Fig. 1(c). On the other hand, comparing Fig. 1(a) and Fig. 1(b), the locations of U2 are considered to be quite different since U2's RSRP from FAP2-FAP4 in the two cases have weak correlation. Therefore, even though RSRP statistics from FAP1 are very different in the two cases, we cannot infer whether FAP1 experiences outage or not. Based on the above analysis, we observe that an FAP can check the states of neighboring FAPs by comparing current statistics with historical statistics in normal cases.

Based on this observation, we can tackle the vertical handover issue and enable the distributed trigger mechanism. In the trigger mechanism, each femtocell monitors the state of its neighboring femtocells based on correlations between current RSRP statistics and historical RSRP statistics reported by the users. Moreover, multiple femtocells can cooperatively process RSRP statistics by further exploiting the correlations over a period of time to cope with the user statistic sparsity issue.

C. COD Architecture Overview

The goal of COD is to detect outaged femtocells accurately and efficiently by meeting the requirements discussed in Section III-A. To achieve this goal, two stages are involved: a distributed trigger stage with no inter-cell communications, and a cooperative detection stage with high accuracy and little delay. In the trigger stage, each FAP collects the user-reported RSRP statistics and sends the MBS a trigger message if current statistics are abnormal. Then, the MBS initiates the detection stage and makes a final decision based on RSRP statistics collected from multiple FAPs within the cooperation range.

Fig. 2 illustrates the COD architecture. Before the trigger stage, each FAP stores a copy of *benchmark data* beforehand, which is collected when all FAPs are normal. Benchmark data contains the RSRP statistics from all neighboring FAPs in the form of a matrix **R**, where element $R_{u,f}$ in **R** is the RSRP of user u from FAP f. In the trigger stage, each FAP runs the trigger algorithm to monitor the states of neighboring femtocells by checking the reported RSRP statistics from its associated users. To check whether the RSRP statistics are normal or not, the FAP predicts the expected normal RSRP statistics based on the benchmark data via collaborative filtering. As for an FAP

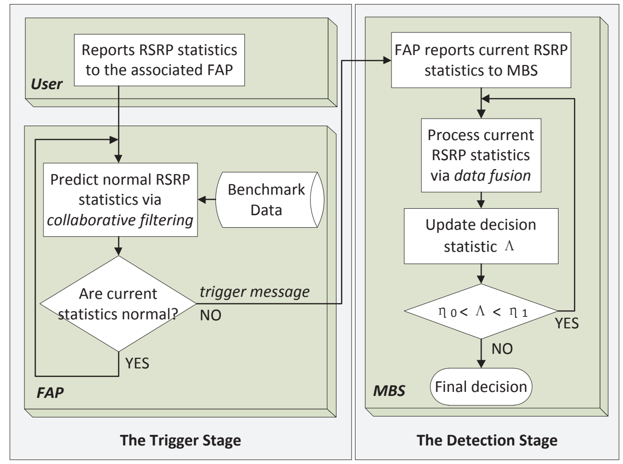

Fig. 2: Architecture overview

i, if the RSRP statistics from a neighboring FAP f deviate from the predicted normal statistics, then FAP i will send a trigger message to the MBS to trigger the detection stage to further decide whether the FAP f experiences outage.

In the detection stage, all the FAPs within the cooperation range report the statistics collected in trigger stage to the MBS periodically until the MBS collects enough information for making a final decision. In each iteration, based on the newly reported RSRP statistics, the MBS processes the statistics via data fusion to update decision statistic, and compares it with pre-computed thresholds (i.e. η_0 and η_1), until it is qualified to make a final decision. The thresholds are computed to guarantee the pre-defined false alarm and misdetection rates. If the decision statistic is below the lower threshold (i.e. η_0), the MBS makes a final decision that FAP f experiences outage. If the decision statistic is above the higher threshold (i.e. η_1), the MBS decides that FAP f is normal. Otherwise, the MBS continues to take another round and accumulates more RSRP statistics.

IV. Collaborative Filtering-Based Trigger Mechanism

The trigger stage contains two steps, namely, the normal RSRP statistics prediction and the trigger decision, as illustrated in Fig. 2. To predict normal RSRP statistics, we leverage collaborative filtering to explore the correlations among the femtocell users. Collaborative filtering is originally used in recommendation systems to compare a user's flavor to some reference users' flavors based on their rated items, so as to predict the rating of that user on a certain item. Treating users as rows and items as columns, the ratings form a matrix. Then, collaborative filtering aims to reconstruct a matrix with missing entries by exploiting correlations across different rows. We can consider the femtocell users as users in a recommendation system, the FAPs as items, RSRP statistics as ratings and the benchmark data as the flavor data of reference users. Similar to the recommendation systems, we leverage collaborative filtering to predict the RSRP statistic from a target FAP based on the benchmark data matrix. Since the benchmark data is collected in normal cases, the predicted RSRP statistic is the expected normal RSRP statistic. If the predicted RSRP statistic and the collected RSRP statistic are significantly different, the target FAP is very likely in an outaged state. Based on this intuition, we design a trigger mechanism as follows.

A. Normal RSRP Statistics Prediction

1) Collaborator Selection: To make a trigger decision, the expected normal RSRP $r_{u,f}$ of a user u from the target FAP f needs to be estimated. The first step is to select users in the benchmark data for correlation computation. In femtocell networks, only nearby users have strong spatial correlations, while computing correlations with remote users will involve large errors due to shadowing fading and multi-path fading. Thus, we select a set of users that can receive the signals from the FAP associated with u, which is denoted as *collaborator set* $C(u)$.

2) Collaborative Prediction: Given the set of collaborators $C(u)$, we need to compute the *interpolation weight* $w_{u,v}|v \in C(u)$ that enables the optimal prediction rule:

$$\hat{r}_{u,f} = \sum_{v \in C(u)} w_{u,v} r_{v,f}, \tag{3}$$

where $\hat{r}_{u,f}$ is the prediction of u's normal RSRP from f, $w_{u,v}$ the interpolation weight, and $r_{v,f}$ the user v's RSRP from f in the benchmark data.

To estimate the interpolation weights, we formulate a suitable optimization problem. Since $r_{u,f}$ is the target statistic that we want to predict, we treat $r_{u,f}$ as a missing entry and use statistics from all the other FAPs to compute the interpolation weights. The objective is to minimize the sum of squared errors for predicting the statistics of u (except $r_{u,f}$). The interpolation weights are learned by modeling the correlations between u and benchmark users through a least squares problem as follows:

$$\min_{w} \sum_{i \neq f} (r_{u,i} - \sum_{v \in C(u)} w_{u,v} r_{v,i})^2. \tag{4}$$

The reason for excluding f in Eq. (4) is that f is the target FAP to be predicted, which is considered as abnormal. The optimal solution to the least squares problem (4) can be achieved by differentiation as a solution of linear system of equations. The optimal weights are given by:

$$\mathbf{w}^* = \left(\mathbf{R}^T \mathbf{R}\right)^{-1} \mathbf{R}^T \mathbf{U}, \tag{5}$$

where $\mathbf{w}^*$ is the optimal weights vector defined by $w_v^* = w_{u,v}$, $\mathbf{R}$ the benchmark users' RSRP matrix defined by $R_{v,i} = r_{v,i}$, and $\mathbf{U}$ the user u's RSRP vector defined by $U_j = r_{u,j}$. Based on the estimation of $\mathbf{w}^*$, the prediction of the current normal RSRP is computed according to Eq. (3).

B. Trigger Decision

After computing $\hat{r}_{u,f}$, the trigger decision is made based on maximum likelihood rule. In particular, $\hat{r}_{u,f}$ is treated as the mean of normal hypothesis $\mathcal{H}_0$ as defined in Eq. (2), the noise power N_o as the mean of normal hypothesis $\mathcal{H}_0$, and the actual current RSRP $r_{u,f}$ as test statistic. If the probability of $r_{u,f}$ under $\mathcal{H}_0$ is larger than the probability of $r_{u,f}$ under $\mathcal{H}_1$, the detection stage is triggered. Otherwise, FAP runs the trigger procedure over again on the newly arrived RSRP statistics.

V. Sequential Cooperative Detection via Data-Fusion

In this section, we first formulate the cooperative detection problem in the detection stage as a sequential hypothesis testing problem. Then, we derive the closed-form expression of average detection delay by approximating the test statistics. Finally, based on the closed-form expression of average detection delay, we analyze the impacts of several system parameters on the performance of the cooperative outage detection.

A. Sequential Hypothesis Testing

We assume that the detection for FAP f is triggered. The vector of test statistics collected in detection round t is denoted as $\boldsymbol{\theta}_t = [r_{1_t}, ..., r_{i_t}, ..., r_{n_t}]^T$, where r_{i_t} is the user i's RSRP from f in detection round t. n_t is the number of users within the cooperation range R centered by the location of f. As shown in Eq. (2), the RSRP statistics can be approximated as a Gaussian distribution in both normal and outage cases. Thus, our outage detection problem is a binary decision problem for deciding whether hypothesis $\mathcal{H}_0$ or $\mathcal{H}_1$ is true, given the test statistics $\boldsymbol{\theta}$, where $\boldsymbol{\theta} = [{\boldsymbol{\theta}_1}^T, ..., {\boldsymbol{\theta}_t}^T, ..., {\boldsymbol{\theta}_T}^T]$.

To solve the binary decision problem, the MBS keeps collecting new test statistics from users until the amount of information and the resulting testing performance are satisfied. To achieve this goal, we take Wald's *Sequential Probability Ratio Test* (SPRT) [15] as the data processing rule to decide the stopping time of making a final decision. The main advantage of SPRT is that it requires the minimal number of test statistics to achieve the same error probability, which is attained at the expense of additional computation. In the sequential decision process, the MBS computes the log likelihood ratio and compares it with two thresholds η_0 and η_1. It either determines on one of the two hypothesis, or decides to make another round of statistics collection.

The likelihood ratio in detection round t is defined by:

$$\lambda_t \triangleq \ln \frac{p(\boldsymbol{\theta}_t|\mathcal{H}_1)}{p(\boldsymbol{\theta}_t|\mathcal{H}_0)}, \tag{6}$$

where $p(\boldsymbol{\theta}_t|\mathcal{H}_k)$ is the joint probability density function (p.d.f.) of test statistics collected in detection round t under the hypothesis $\mathcal{H}_k$ $(k = 0, 1)$. Note that test statistics are assumed to be i.i.d. and follow the Gaussian distribution described in Eq. (2). Thus, Eq. (6) can be written as:

$$\lambda_t = \ln \frac{p(r_{1_t}, ..., r_{n_t}|\mathcal{H}_1)}{p(r_{1_t}, ..., r_{n_t}|\mathcal{H}_0)} = \sum_{i_t=1}^{n_t} \ln \frac{p(r_{i_t}|\mathcal{H}_1)}{p(r_{i_t}|\mathcal{H}_0)}, \tag{7}$$

where r_{i_t} is approximated as $r_{i_t} \sim \mathcal{N}(\mu_k, \sigma_k)$ under the hypothesis $\mathcal{H}_k$, according to the CLT. Note that ${\sigma_0}^2 = \frac{{N_o}^2}{M}$ and ${\sigma_1}^2 = \frac{P_u+{N_o}^2}{M}$, where P_u and N_o are the average received signal power at users and the noise power. In a very low SNR environment, it is reasonable to approximate (P_u+N_o) as N_o, and hence $\sigma_1 \approx \sigma_0$. Then, Eq. (7) can be expressed as:

$$\lambda_t = \frac{(\mu_1 - \mu_0)\sum_{i_t=1}^{n_t} r_{i_t} + \frac{1}{2}\sum_{i_t=1}^{n_t}({\mu_0}^2 - {\mu_1}^2)}{{\sigma_0}^2}. \tag{8}$$

The next step is to determine the decision statistic Λ_T in detection round T. Λ_T is defined to be the joint likelihood ratio of a sequential test statistics $\boldsymbol{\theta}_1, ..., \boldsymbol{\theta}_T$:

$$\Lambda_T \triangleq \ln \frac{p(\boldsymbol{\theta}_1, ..., \boldsymbol{\theta}_T|\mathcal{H}_1)}{p(\boldsymbol{\theta}_1, ..., \boldsymbol{\theta}_T|\mathcal{H}_0)}, \tag{9}$$

where $p(\boldsymbol{\theta}_1, ..., \boldsymbol{\theta}_T|\mathcal{H}_k)$ is the joint p.d.f. of test statistics under $\mathcal{H}_k$). Regarding that the test statistics are Gaussian and i.i.d., we have:

$$\Lambda_T = \sum_{t=1}^{T} \ln \frac{p(\boldsymbol{\theta}_t|\mathcal{H}_1)}{p(\boldsymbol{\theta}_t|\mathcal{H}_0)} = \sum_{t=1}^{T} \lambda_t, \tag{10}$$

and based on Eqs. (8) and (11), we further derive Λ_T as follows:

$$\Lambda_T = \frac{(\mu_1 - \mu_0)}{{\sigma_0}^2} \sum_{t=1}^{T}\sum_{i_t=1}^{n_t} r_{i_t} + \frac{1}{2{\sigma_0}^2}\sum_{t=1}^{T}\sum_{i_t=1}^{n_t}({\mu_0}^2 - {\mu_1}^2). \tag{11}$$

The decision of SPRT in detection round T is based on the following rules [15]:

$$\begin{cases} \Lambda_T \geq \eta_1 & \Rightarrow \text{accept } \mathcal{H}_1 \\ \Lambda_T \leq \eta_0 & \Rightarrow \text{accept } \mathcal{H}_0 \\ \eta_0 < \Lambda_T < \eta_1 & \Rightarrow \text{take another detection round,} \end{cases} \tag{12}$$

where η_1 and η_0 are the detection thresholds, which are determined by the predefined values of desired false alarm rate α and misdetection rate β. However, the outage detection problem is opposite to the detection problem described in [15] in the sense of misdetection rate and false alarm rate, since $\mathcal{H}_0$ is hypothesis for outage occurrence while $\mathcal{H}_1$ for event occurrence in [15]. Thus, the detection thresholds are given by:

$$\eta_1 = \ln \frac{1-\alpha}{\beta} \text{ and } \eta_0 = \ln \frac{\alpha}{1-\beta}. \tag{13}$$

where α and β are the desired false alarm rate and misdetection rate, respectively. Note that the actual achievable false alarm and misdetection rates could be higher than α and β [20], which is shown in our simulation results.

B. Average Detection Delay Analysis

The aim of SPRT is to achieve the desired false alarm and misdetection rates with the minimal number of detection rounds, which stands for detection delay. The expected number of detection rounds is computed according to [15]:

$$\mathbb{E}[\Lambda_T] = \mathbb{E}[T] \times \mathbb{E}[\lambda_t]. \tag{14}$$

First, we derive the expectation of Λ_T in normal cases, namely, under hypothesis $\mathcal{H}_1$. According to (12), $\mathcal{H}_1$ is accepted when Λ_T reaches the threshold η_1, otherwise $\mathcal{H}_2$ is accepted (i.e., false alarm). Thus, Λ_T reaches the threshold η_0 with the probability of false alarm rate α and reaches the threshold η_1 with probability $(1-\alpha)$. Then, according to Eq. (13), we derive the expectation of Λ_T under $\mathcal{H}_1$:

$$\mathbb{E}[\Lambda_T|\mathcal{H}_1] = (1-\alpha)\ln\frac{1-\alpha}{\beta} + \alpha \ln \frac{\alpha}{1-\beta}. \tag{15}$$

Similarly, we derive the expectation of Λ_T under $\mathcal{H}_0$:

$$\mathbb{E}[\Lambda_T|\mathcal{H}_0] = \beta\ln\frac{1-\alpha}{\beta} + (1-\beta) \ln \frac{\alpha}{1-\beta}. \tag{16}$$

Next, according to Eq. (8), the expectation of λ_t under $\mathcal{H}_k$ can be expressed as:

$$\mathbb{E}[\lambda_t|\mathcal{H}_k] = \frac{(\mu_1 - \mu_0)\mathbb{E}[\sum_{i_t=1}^{n_t} r_{i_t}^k] + \frac{1}{2}\mathbb{E}[\sum_{i_t=1}^{n_t}({\mu_0}^2 - {\mu_1}^2)]}{{\sigma_0}^2}, \tag{17}$$

where $r_{i_t}^k$ is RSRP from the FAP we are detecting under hypothesis $\mathcal{H}_k$.

According to Eqs. (15) (16) and (17), we derive the average detection rounds in normal cases:

$$\mathbb{E}[T|\mathcal{H}_1] = \frac{{\sigma_0}^2(1-\alpha)\ln\frac{1-\alpha}{\beta} + {\sigma_0}^2\alpha\ln\frac{\alpha}{1-\beta}}{(\mu_1 - \mu_0)\mathbb{E}[\sum_{i_t=1}^{n_t} r_{i_t}^1] + \frac{1}{2}\mathbb{E}[\sum_{i_t=1}^{n_t}({\mu_0}^2 - {\mu_1}^2)]}, \tag{18}$$

and the average detection rounds in outage cases:

$$\mathbb{E}[T|\mathcal{H}_0] = \frac{{\sigma_0}^2\beta\ln\frac{1-\alpha}{\beta} + {\sigma_0}^2(1-\beta)\ln\frac{\alpha}{1-\beta}}{(\mu_1 - \mu_0)\mathbb{E}[\sum_{i_t=1}^{n_t} r_{i_t}^0] + \frac{1}{2}\mathbb{E}[\sum_{i_t=1}^{n_t}({\mu_0}^2 - {\mu_1}^2)]}. \tag{19}$$

To further analyze the impacts of cooperation range, FAP transmission power, and user density, we need to derive the expectation of the sum of test statistics $\mathbb{E}[\sum_{i_t=1}^{n_t} r_{i_t}^k]$, which, however, has no closed-form expression. Thus, we approximate the test statistics as follows.

We first approximate $\mathbb{E}[\sum_{i_t=1}^{n_t} r_{i_t}^1]$. Note that test statistics follow the Gaussian distribution as described in Eq. (2). The expected sum of test statistics under $\mathcal{H}_1$ can be written as:

$$\mathbb{E}\left[\sum_{i_t=1}^{n_t} r_{i_t}^1\right] = \mathbb{E}\left[\sum_{i_t=1}^{n_t} r_{i_t}\mathcal{N}\left(P_{i_t} + N_o, {\sigma_0}^2\right)\right], \tag{20}$$

where P_{i_t} is the received signal strength from the FAP we are detecting. In practice, the measurement error (i.e., ${\sigma_0}^2$) is much smaller than RSRP. Thus, we can approximate Eq. (20)

as follows:

$$\begin{aligned}\mathbb{E}\left[\sum_{i_t=1}^{n_t} r_{i_t}^1\right] \approx& \mathbb{E}\left[\sum_{i_t=1}^{n_t} P_{i_t}\right] + \mathbb{E}\left[\sum_{i_t=1}^{n_t} N_o\right] \\ =& P_o\mathbb{E}\left[\sum_{i_t=1}^{n_t}\left(\frac{d_o}{d_{i_t}}\right)^a e^{X_{i_t}} e^{Y_{i_t}}\right] + N_o\mathbb{E}[n_t] \\ =& P_o\mathbb{E}\left[\sum_{i_t=1}^{n_t}\left(\frac{d_o}{d_{i_t}}\right)^a\right]\mathbb{E}\left[e^X\right]\mathbb{E}\left[e^Y\right] \\ &+ N_o\mathbb{E}[n_t], \end{aligned} \tag{21}$$

where P_o is FAP's transmission power in normal cases, $(\frac{d_o}{d_{i_t}})^a$ the user i's channel gain from path loss at time t, e^X and e^Y the shadowing fading factor and multi-path fading factor, respectively. According to [21], the sum of interference of transmitters with a Poisson distribution to a receiver can be approximated as a log-normal distribution. Correspondingly, we can approximate the sum of the received FAP signal strengths at users with Poisson distribution as a log-normal distribution in a similar way. Thus, we have:

$$\mathbb{E}\left[\sum_{i_t=1}^{n_t}\left(\frac{d_o}{d_{i_t}}\right)^a\right] \sim \mathit{Log}\text{-}\mathcal{N}(\mu_m, \sigma_m^2), \tag{22}$$

where μ_m and σ_m^2 are given by [21]:

$$\mu_m = \frac{1}{2}\ln\left(\frac{m_1^4}{m_1^2 + m_2}\right) \text{ and } \sigma_m^2 = \ln\left(\frac{m_1^2 + m_2}{m_1^2}\right), \tag{23}$$

where m_k $(k = 1, 2)$ is the kth cumulant of $\sum_{i_t=1}^{n_t}(\frac{d_o}{d_{i_t}})^a$ given as:

$$m_k = \frac{2\rho\pi d_o^{ka}}{ka - 2}\left(\frac{1}{\epsilon^{ka-2}} - \frac{1}{R^{ka-2}}\right), \tag{24}$$

where ρ is the user density, ϵ the minimum separation between a user and an FAP, and R the cooperation range. Only users within R will report their RSRP statistics to the MBS. In femtocell networks, we have $ka - 2 > 0$ and $\epsilon \ll R$. Thus, m_k can be approximated as:

$$m_k \approx \frac{2\rho\pi d_o^{ka}}{(ka-2)\epsilon^{ka-2}}. \tag{25}$$

By far, we derive all the expectations that are needed to compute the sum of test statistics, i.e., $\mathbb{E}[\sum_{i_t=1}^{n_t}(\frac{d_o}{d_{i_t}})^a] = e^{\mu_m + \frac{1}{2}\sigma_m}$, $\mathbb{E}[e^X] = e^{\frac{1}{2}\sigma}$, $\mathbb{E}[e^Y] = 1$ and $\mathbb{E}[n_t] = \rho\pi R^2$. Finally, $\mathbb{E}[T|\mathcal{H}_1]$ can be derived as:

$$\mathbb{E}[T|\mathcal{H}_1] = \frac{{\sigma_0}^2(1-\alpha)\ln\frac{1-\alpha}{\beta} + {\sigma_0}^2\alpha\ln\frac{\alpha}{1-\beta}}{(\mu_1 - \mu_0)\rho\pi\left(\left(N_o - \frac{\mu_1+\mu_0}{2}\right)R^2 + \frac{2P_o d_o^a e^{\frac{1}{2}\sigma^2}}{(a-2)\epsilon^{a-2}}\right)}. \tag{26}$$

Similarly, we derive $\mathbb{E}[T|\mathcal{H}_0]$ as follows. According to Eq. (2), $\mathbb{E}[\sum_{i_t=1}^{n_t} r_{i_t}^1]$ can be expressed as:

$$\mathbb{E}[\sum_{i_t=1}^{n_t} r_{i_t}^0] = \mathbb{E}[\sum_{i_t=1}^{n_t} r_{i_t}\mathcal{N}(N_o, {\sigma_0}^2)] = N_o\rho\pi R^2. \tag{27}$$

Then, we derive $\mathbb{E}[T|\mathcal{H}_0]$ as:

$$\mathbb{E}[T|\mathcal{H}_0] = \frac{{\sigma_0}^2\beta\ln\frac{1-\alpha}{\beta} + {\sigma_0}^2(1-\beta)\ln\frac{\alpha}{1-\beta}}{\left(N_o - \frac{\mu_1+\mu_0}{2}\right)(\mu_1 - \mu_0)\rho\pi R^2}. \tag{28}$$

Since α and β are predefined, we have the following observation based on Eq. (28):

Proposition 1: The average outage detection delay is inversely proportional to the user density and the cooperation area (i.e. $\rho\pi R^2$), but is independent of the FAP's transmission power. ■

VI. Numerical Results

In this section, we demonstrate the performance of COD, and the impacts of some system parameters on the detection accuracy and delay with simulation results.

A. Simulation Setup

We consider a two-tier cellular network comprised of multiple femtocells overlaid on a macrocell. Femtocells are distributed randomly within an area of 1000 m $\times$ 1000 m. All FAPs use a uniform transmission power and operate at the carrier frequency of 2.5 GHz with 5 MHz channel bandwidth [22]. Femtocell users are distributed randomly within the same area, and are associated with the FAP with the strongest RSRP. Users send their RSRP reports every 0.1 s. Each femtocell user moves according to the random waypoint mobility model [23] within the range of the network area. Each user moves with speed interval of [0,10] m/s, pause time interval of [0,1] s, and walk interval of [2,6] s. The thermal noise power and the minimal sensible signal strength are set to -107.5 dBm, and the path loss exponent a is set to 4. The misdetection rate and false alarm rate parameters $\alpha = \beta = 0.01$. Unless explicitly otherwise stated, the numbers of FAPs and users are 100 and 1000, respectively, the FAP transmission power $P_o = 5$ dBm, cooperation range $R = 600$ m, and the standard deviation of the shadowing fading dB-spread $\sigma_{dB} = 8$ dB [22], where $\sigma_{dB} = 10\sigma/\ln(10)$. The simulation results are the average results from 5000 randomly generated network topologies.

To demonstrate the merits of the proposed statistic correlation based architecture, we compare COD with the commonly used maximum likelihood ratio based approach [24] referred to as MAJ. In MAJ, each user associated with the femtocell in normal state collects RSRP statistics, decides a binary hypothesis problem based on the maximum likelihood ratio, and reports the binary decision directly to the MBS. Then, the MBS makes the decision by majority vote. For a fair comparison, we enhance MAJ by collecting test statistics of the same number of detection rounds with COD. Thus, these two schemes have the same detection delay.

B. Overall Performance

Fig. 3 and Fig. 4 illustrate the overall performance of COD, i.e., detection accuracy and detection delay. Detection accuracy is defined to be the probability of correctly detecting an outaged femtocell. Note that we do not show false alarm rate

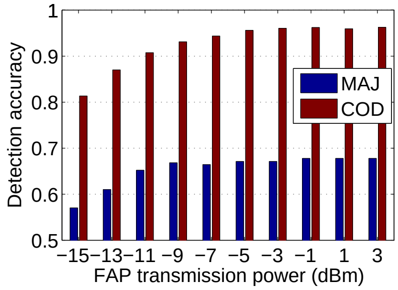

Fig. 3: Overall performance: detection accuracy

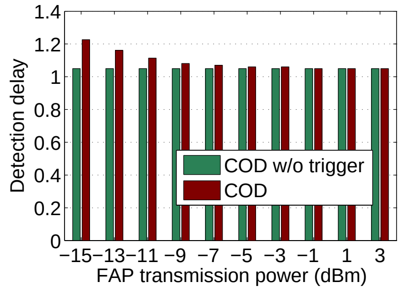

Fig. 4: Overall performance: detection delay

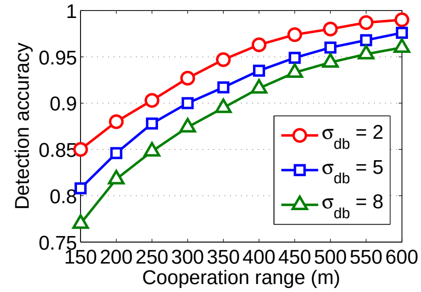

Fig. 5: Impact of cooperation range on detection accuracy

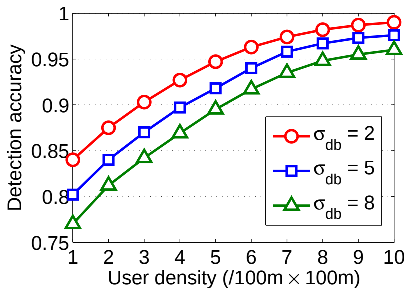

Fig. 6: Impact of user density on detection accuracy

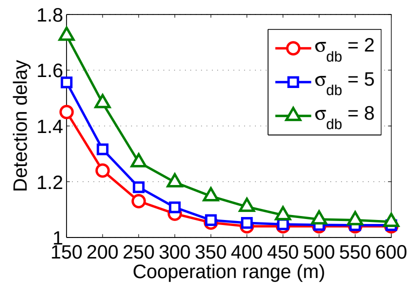

Fig. 7: Impact of cooperation range on detection delay

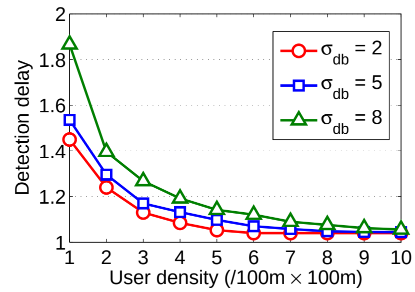

Fig. 8: Impact of user density on detection delay

in the figures since it is less than 0.001 in all cases, which is much higher than misdetection rate. Detection delay is defined as the number of detection rounds.

Fig. 3 depicts the detection accuracy for various FAP power levels, and it is shown that COD outperforms MAJ in detection accuracy by more than 20% in all cases demonstrated. The reason is that COD exploits spatial correlations by collaborative filtering and data fusion to obtain more information for the final decision, while MAJ simply aggregates statistics by majority vote. We observe that both COD and MAJ detect outaged femtocells with higher accuracy as the FAP power increases. This is because when FAP transmission power increases, the gap between the RSRP statistics in normal cases and RSRP statistics in outage cases is larger, making it easier to differentiate these two cases.

Fig. 4 indicates that the difference in the detection delays of COD without trigger stage and COD approaches zero when FAP transmission power increases. The reason is that as the FAP power gets larger, it is easier to differentiate outage cases from normal cases, the probability of immediately triggering the detection stage is higher. We also observe that the detection delay of COD without trigger is independent of the FAP transmission power, which matches our analytical results (Proposition 1).

C. Impacts of Parameters on Detection Accuracy

Fig. 5 and Fig. 6 show the impacts of parameters on the detection accuracy. As depicted in Fig. 5, COD achieves higher accuracy when cooperation range is larger, which is consistent with Proposition 1. This is because with lager cooperation range, there are more statistics contributed to cooperative detection, and thus the spatial correlations are better exploited.

Fig. 6 indicates that the detection accuracy goes higher when user density increases, which is consistent with Proposition 1. The reason is that higher user density enables better spatial correlation exploitation. It can also be seen in both Fig. 5 and Fig. 6 that the detection accuracy is slightly lower with larger σ_{dB}. This is because larger σ_{dB} implies more severe shadowing fading, which results in statistics with larger randomness.

D. Impacts of Parameters on Detection Delay

The impacts of parameters on the detection delay depicted in Fig. 7 and Fig. 8, which match the analytical results in Proposition 1. Fig. 7 and Fig. 8 show that detection delay increases when σ_{dB} is larger but decreases with the increment of the cooperation range or the user density, which can be explained by Eq. (26) and Eq. (28). We can see that with enough cooperation range (e.g., 600m) and reasonably high user density (e.g., $4/100$m $\times 100$m), the detection delay is very small (less than 1.2 rounds) even with severe shadowing fading ($\sigma_{dB} = 8$).

VII. Related Work

The problem we studied in this paper is related to two areas in wireless networks, namely, troubleshooting in cellular networks and wireless LANs, and primary user detection in cognitive radio networks.

In cellular networks, troubleshooting has been studied in previous works [7] [8] [25]. [8] processes historical user statistics via offline Bayesian analysis to diagnose the root causes for the cell outage. Based on a similar but enhanced offline analysis model, [25] further studies the outage troubleshooting problem in the context of femtocell networks. These works focus on offline analysis of the root causes after outage has been detected, while we emphasize the online detection of the outaged cell. The only online detection approach is proposed in [7], which detects outaged macrocells based on user's neighbor cell list reports. In wireless LANs, there have been a lot of studies on node failure and faults detection problems [12] [13]. [13] is the first study on fault detection and diagnosis in the IEEE 802.11 infrastructure wireless networks. In [13], the *client conduit* protocol is proposed to allow clients to cooperatively identify the root cause of disconnection issues. A fault management system is designed in [12] to cooperate to automatically detect fault nodes and troubleshoot network problems, in which the detection procedure is triggered only when a client is disconnected from AP. However, these outage or fault detection approaches cannot be applied in the femtocell outage detection scenario due to the unique challenges listed in Section I.

In cognitive radio networks, primary user detection [26] [27] is also related to our work. These works focus on detecting the signals of primary users by spectrum sensing. The fundamental differences between these works and our work are twofold. First, the issues caused by the two-tier architecture of femtocells are not involved in these works. Second, the communication overhead is more strictly constrained in femtocell outage detection since femtocell should guarantee quality of service for the users in the first place.

VIII. Conclusions

This paper proposes a cooperative detection architecture called COD for cell outage detection in femtocell networks, which addresses the unique challenges of femtocell networks. COD contains a trigger stage and a detection stage. By exploiting the spatial correlations of RSRP statistics via collaborative filtering, the trigger mechanism enables COD to trigger the detection stage without extra inter-cell communications. In the detection stage, we model the detection problem as hypothesis testing, and derive closed-form expressions of detection delay. Our evaluations show that our cooperative detection largely reduces communication overhead and achieves higher detection accuracy than the existing approach under the same delay condition.

Acknowledgement

The research was supported in part by grants from RGC under the contracts CERG 623209 and 622410, HKUST grant SRFI11FYT01, the grant from Huawei-HKUST joint lab, and the National Natural Science Foundation of China under Grants No. 60933012.

References

[1] "Telecommunication management; self-organizing networks (SON) policy network resource model (NRM) integration reference point (IRP); information service (IS)." 3GPP TS 32.522, Rel. 9, Mar. 2010.

[2] "Telecommunication management; self-organizing networks (SON); self-healing concepts and requirements." 3GPP TS 36.902, Rel. 10, Aug. 2010.

[3] R. Combes, Z. Altman, and E. Altman, "Self-organization in wireless networks: A flow-level perspective," in *Proc. IEEE INFOCOM*, Mar. 2012, pp. 2946 –2950.

[4] A. Stolyar and H. Viswanathan, "Self-organizing dynamic fractional frequency reuse for best-effort traffic through distributed inter-cell coordination," in *Proc. IEEE INFOCOM*, Apr. 2009, pp. 1287 –1295.

[5] M. Amirijoo *et al.*, "Cell outage management in lte networks." COST 2100 TD(09)941, Sep. 2009.

[6] "Self-organizing networks, NEC's propoals for next-generalization radio network management." NEC White Paper, 2009.

[7] C. Mueller, M. Kaschub, C. Blankenhorn, and S. Wanke, "A cell outage detection algorithm using neighbor cell list reports," *International Workshop on Self-Organizing Systems*, pp. 218–229, 2008.

[8] R. Khanafer *et al.*, "Automated diagnosis for UMTS networks using bayesian network approach," *IEEE Trans. Veh. Technol.*, vol. 57, no. 4, pp. 2451 –2461, Jul. 2008.

[9] "3G Home NodeB (HNB) study item." 3GPP TR 25.820, Mar. 2008.

[10] V. Chandrasekhar, J. Andrews, and A. Gatherer, "Femtocell networks: a survey," *IEEE Commun. Magazine*, vol. 46, no. 9, pp. 59 –67, Sep. 2008.

[11] "Evolved Universal Terrestrial Radio Access Network (E-UTRAN); physical layer - measurements." 3GPP TS 36.214, Dec. 2008.

[12] R. Chandra, V. N. Padmanabhan, and M. Zhang, "Wifiprofiler: cooperative diagnosis in wireless LANs," in *Proc. ACM MobiSys*, 2006, pp. 205–219.

[13] A. Adya, P. Bahl, R. Chandra, and L. Qiu, "Architecture and techniques for diagnosing faults in ieee 802.11 infrastructure networks," in *Proc. ACM MobiCom*, 2004, pp. 30–44.

[14] D. Goldberg, D. Nichols, B. M. Oki, and D. Terry, "Using collaborative filtering to weave an information tapestry," *Commun. ACM*, vol. 35, pp. 61–70, Dec. 1992.

[15] A. Wald, "Sequential tests of statistical hypotheses," *Ann. Math. Statist.*, vol. 16, no. 2, pp. 117–186, 1945.

[16] V. Erceg *et al.*, "An empirically based path loss model for wireless channels in suburban environments," *IEEE J. Sel. Areas Commun.*, vol. 17, no. 7, pp. 1205–1211, 1999.

[17] S. Shellhammer *et al.*, "Performance of power detector sensors of DTV signals in IEEE 802.22 WRANs," in *Proc. ACM TAPAS*, 2006.

[18] D. Fan, Z. Feng, L. Tan, V. Le, and J. Song, "Distributed self-healing for reconfigurable WLANs," in *Proc. IEEE WCNC*, Apr. 2010, pp. 1 –6.

[19] X. Chen, J. Huang, and H. Li, "Adaptive channel recommendation for dynamic spectrum access," in *Proc. IEEE DySPAN*, May 2011, pp. 116 –124.

[20] P. Varshney and C. Burrus, *Distributed detection and data fusion*. Springer Verlag, 1997.

[21] R. Menon, R. Buehrer, and J. Reed, "On the impact of dynamic spectrum sharing techniques on legacy radio systems," *IEEE Trans. Wireless Commun.*, vol. 7, no. 11, pp. 4198 –4207, Nov. 2008.

[22] J.-H. Yun and K. G. Shin, "Ctrl: a self-organizing femtocell management architecture for co-channel deployment," in *Proc. ACM MobiCom*, Sep. 2010, pp. 61–72.

[23] C. Bettstetter, G. Resta, and P. Santi, "The node distribution of the random waypoint mobility model for wireless ad hoc networks," *IEEE Trans. Mobile Computing*, vol. 2, no. 3, pp. 257 – 269, Jul.-Sep. 2003.

[24] H. Akaike, "Information theory and an extension of the maximum likelihood principle," in *Proc. IEEE ISIT*, Jul. 1973, pp. 267–281.

[25] W. Wang, J. Zhang, and Q. Zhang, "Transfer learning based diagnosis for configuration troubleshooting in self-organizing femtocell networks," in *Proc. IEEE GLOBECOM*, Dec. 2011, pp. 1–5.

[26] R. Chen, J.-M. Park, and K. Bian, "Robust distributed spectrum sensing in cognitive radio networks," in *Proc. IEEE INFOCOM*, Apr. 2008, pp. 1876 –1884.

[27] A. Min, X. Zhang, and K. Shin, "Spatio-temporal fusion for small-scale primary detection in cognitive radio networks," in *Proc. IEEE INFOCOM*, Mar. 2010, pp. 1 –5.